Influence of obesity and insulin sensitivity on insulin signaling genes in human omental and subcutaneous adipose tissue[S]

R. MacLaren,*,† W. Cui,*,† S. Simard,† and K. Cianflone[1,*,†]

Experimental Medicine,* McGill University Health Centre, Montreal, Canada; and Centre de Recherche Hôpital Laval,† Laval University, Quebec, Canada

Abstract Obesity and insulin resistance are independent risk factors for metabolic syndrome, diabetes, and cardiovascular disease. Adipose tissue samples from nonobese (NO), insulin-sensitive obese (ISO), and insulin-resistant obese (IRO) subjects from subcutaneous (SC) and omental (OM) adipose tissue (n = 28) were analyzed by microarray and confirmed by real-time PCR. Insulin signaling gene expression changes were greater in OM than in SC tissue and were related to insulin resistance rather than to obesity; few genes correlated with body mass index. Insulin receptor and insulin receptor substrate 1 (IRS-1) increased in the IRO versus pooled insulin-sensitive (NO+ISO) subjects. In glucose transport, PI3Kα and PDK2 decreased in IRO subjects, whereas PI3Kγ, Akt2, GLUT4, and GLUT1 increased. IRS-1 regulators Jnk and IKK increased in IRO ($P < 0.01$ and $P < 0.001$ respectively). In protein synthesis, most genes examined were downregulated in IRO subjects, including mTor, Rheb, and 4EBP and eIF members (all $P < 0.05$). In proliferation, SHC, SOS, and Raf1 ($P < 0.05$) were increased, whereas Ras and MEK1/2 kinase 1 ($P < 0.05$) were decreased, in IRO subjects. Finally, in differentiation, PPARγ, CEBPα, and CEBPβ decreased, whereas PPARδ, CEBPγ, and CEBPε increased, in IRO subjects ($P < 0.05$). Together, microarray and real-time PCR data demonstrate that insulin resistance rather than obesity is associated with altered gene expression of insulin signaling genes, especially in OM adipose tissue.—MacLaren, R., W. Cui, S. Simard, and K. Cianflone. **Influence of obesity and insulin sensitivity on insulin signaling genes in human omental and subcutaneous adipose tissue. *J. Lipid Res.* 2008.** 49: **308–323.**

Supplementary key words differentiation • glucose • proliferation • protein synthesis • insulin-sensitive obese • insulin-resistant obese

Obesity and insulin resistance have both been identified as independent risk factors for metabolic syndrome, diabetes, and cardiovascular disease (1, 2). Many studies have focused on the physiologic parameters and genetic predisposition of subjects presenting with both obesity and insulin resistance (3). It was recently brought to attention, however, that subsets of obese individuals remain relatively insulin-sensitive (4–6). In the literature, they are referred to as insulin-sensitive obese (ISO) (7), metabolically healthy but obese (8), and metabolically normal but obese (9) subjects. For consistency, we use the term ISO throughout the present discussion. A number of studies have been conducted to identify physiologically different characteristics of the ISO population (10). In addition to insulin sensitivity, ISO subjects have lower plasma triglycerides and higher HDL cholesterol (9, 11). Shin et al. (12) determined that circulating C-reactive protein, interleukin 6, oxidized LDL, and visceral fat were lower in ISO compared with insulin-resistant obese (IRO) subjects. However, there are few data describing gene regulation that might account for this overall healthier status of ISO individuals.

Adipose tissue is one of the key peripheral targets of insulin; acting as both an endocrine organ and an energy storage depot (13), it can affect whole-body insulin sensitivity. Characteristics of adipose tissue may contribute to an ISO or IRO profile; however, not all depots of adipose tissue are the same. Subcutaneous (SC) and omental (OM) adipose tissue depots have different physiological characteristics. These differences include insulin receptor (InsR) expression (1, 14) and affinity (15), triglyceride synthesis (16), adipokine expression and secretion (17–19), and response to hormones [insulin (14), epinephrine (20), and sex hormones (21)]. Although many studies have compared adipose tissue from nonobese (NO) and

Manuscript received 27 April 2007 and in revised form 14 September 2007 and in re-revised form 1 November 2007.

Published, JLR Papers in Press, November 6, 2007.
DOI 10.1194/jlr.M700199-JLR200

Abbreviations: BMI, body mass index; cRNA, complimentary RNA; FDR, false discovery rate; HOMA-IR, homeostasis model assessment insulin resistance; InsR, insulin receptor; IRO, insulin-resistant obese; IRS-1, insulin receptor substrate 1; ISO, insulin-sensitive obese; NIDDM, non-insulin-dependent diabetes mellitus; NO, nonobese; OM, omental; SAM, Significant Analysis of Microarrays; SC, subcutaneous.

[1] To whom correspondence should be addressed.
e-mail: katherine.cianflone@crhl.ulaval.ca

[S] The online version of this article (available at http://www.jlr.org) contains supplementary data in the form of two tables.

obese subjects for differences in physiological parameters (22, 23) and gene expression (17, 24), comparisons targeting specifically ISO versus IRO subjects in either SC or OM adipose tissue are limited. In fact, although there are a few studies on adipokines in an ISO population (17, 18), to our knowledge there are no studies on insulin signaling gene expression in an ISO population, although insulin is a known regulator of glucose transport, protein synthesis, triglyceride synthesis, growth, and hormone (adipokine) secretion in adipose tissue (25, 26).

The purpose of the present study, therefore, was to comprehensively compare differences in adipose gene expression from NO, ISO, and IRO individuals using both SC and OM adipose tissue samples. We chose to focus on genes related to insulin signaling and associated metabolic processes, including the glucose pathway, protein synthesis, proliferation, and differentiation. We used a 20K microarray to simultaneously measure the expression of many of the key insulin signaling genes in these paths with validation by real-time PCR.

MATERIALS AND METHODS

Subjects

Men and women living in Montreal, Canada, were recruited for this study. Altogether, there were 4 men (2 lean and 2 obese) and 12 women (3 lean and 9 obese). A sample of SC and OM adipose tissue along with a fasting blood sample were collected during surgery. Surgical procedures included bariatric surgery (n = 11), hysterectomy (n = 3), valve replacement (n = 1), and hernia (n = 1). Ethics approval for this project was obtained from the McGill University Heath Centre (Royal Victoria Hospital) ethics review committee (Montreal, Canada), and subjects signed informed consent forms before participation. Of the 16 subjects, none had diabetes or any other known disease (other than the presence of morbid obesity and the single subject with valve replacement). All women were premenopausal. None was taking hypoglycemic or lipid-lowering medication. Body weight was stable at the time of study.

Blood samples

Venous blood samples were collected in the fasting state into nonheparinized and EDTA-free tubes. Samples were collected at 7:00 AM, on the ward after a 12 h fast, before transfer of patients to surgery. Blood samples were centrifuged at 2,000 rpm at 4°C for 10 min and stored at −80°C for later analysis. Insulin levels were measured by RIA (Medicorp, Montreal, Canada). Glucose was measured by colorimetric enzyme assay (GOD-PAP; Roche Diagnostics). Homeostasis model assessment insulin resistance (HOMA-IR) was calculated as follows: fasting insulin (μU/ml) × fasting glucose (mmol/l)/22.5, where insulin (pmol/l)/6.945 = μU/ml. Plasma triglycerides were measured by the GPO-PAP (glycerol phosphate oxidase coupled to phenol and 4-aminophenazone) method and cholesterol was measured by the COD-PAP (cholesterol oxidase coupled to phenol and 4-aminophenazone) method to generate a colorimetric product (Roche Diagnostics). Plasma NEFA concentration was determined by colorimetric enzymatic assay (WAKO Chemicals, Tokyo, Japan). HDL cholesterol concentration was determined using an enzymatic colorimetric assay after precipitation of apolipoprotein B-containing lipoproteins. LDL was calculated using the Friedwald formula [LDL cholesterol = total cholesterol − (triglyceride/2.2) − HDL cholesterol].

Adipose tissue microarray

Adipose tissue was collected at the beginning of the operation (within 30 min) into sterile 50 ml conical tubes and immediately flash-frozen in liquid nitrogen. SC adipose tissue was collected from the SC abdominal wall, and OM adipose tissue was collected from the greater omentum, which is representative of intra-abdominal depots drained by the portal vein. RNA was extracted from the tissue using Qiagen spin columns (Qiagen, Mississauga, Canada) according to the manufacturer's protocol for fatty tissue with the addition of two RNase-free DNase treatments (Qiagen) between RW1 washes. RNA quality was assessed by spectrometry (260:280 ratio) with ratios of 1.9–2.0. As well, RNA quality was assessed by chromatography. Synthesis of complimentary RNA (cRNA) by in vitro transcription and hybridization was performed as described previously (27). Briefly, 10 μg of high-quality total RNA was converted to cDNA and then to biotin-labeled cRNA (10 mM biotin-11-UTP; Perkin-Elmer) by linear amplification (iExpress Assay reagent kit; GE Healthcare Bio-Sciences, Montreal, Quebec). Ten micrograms of labeled cRNA was hybridized to CodeLink UniSet Human 20K I (GE Healthcare Bio-Sciences). The slides were processed according to the manufacturer's instructions and analyzed using Codelink System software (GE Healthcare Bio-Sciences). The spot intensities were median-normalized (signal intensity of probe/median intensity of all discovery probes).

Confirmation by real time PCR

For PCR, 2 μg of RNA was reverse-transcribed to cDNA using the High-Capacity cDNA RT kit (Applied Biosystems, Toronto, Canada) according to the manufacturer's protocols. Confirmation of expression patterns was analyzed by real-time PCR using the delta threshold cycle method with TAQMAN primer/probes (Applied Biosystems) according to the manufacturer's protocol. The primer/probe sets used were as follows: endogenous control B2M (4326319E), insulin receptor substrate 1 (IRS-1) (Hs00178563_m1), PDK2 (Hs00176865_m1), IKK (Hs00989502_m1), mTor (Hs00234522_m1), 4EBP1 (Hs00607050_m1), and CEBPγ (Hs00156454_m1). All primer/probe sets were validated in-house over an exponential range (1:2 to 1:7,500) of cDNA concentrations using a positive control consisting of pooled adipose tissue RNA isolated from human adipose tissue to establish the dynamic range of the assay for each primer/probe specifically in adipose tissue. Detection of the fluorescent signal was quantified by Rotor-Gene 3000 (Corbett Research). This positive control was assayed in each real-time PCR run. For real-time confirmation, a dilution of 1:50 of the cDNA was used in each case, which was linear within the tested exponential range, and all samples (n = 28) were analyzed simultaneously and individually (no samples were pooled).

Statistical analysis

Microarray analysis was conducted using the SAM (for Significant Analysis of Microarrays) procedure (28) version 3.02 available at http://www-stat.stanford.edu/~tibs/SAM. This program is a validated statistical technique for identifying differentially expressed genes across high-density microarrays. This analysis provides a list of significant genes and an estimate of the false discovery rate (FDR), which represents the percentage of genes that could be identified by chance (28). After SAM analysis of SC and OM tissues, we further analyzed the data targeting specific insulin pathways.

Data are expressed using means ± SEM. The cross-nested design was used to analyze three experimental factors: one associated with the comparison between two groups (IRO vs. ISO+NO), fixed factor; one linked to the subjects (nested random factor in group); and one associated with the comparison between results from two different tissues (SC and OM), fixed factor. A mixed-model analysis was performed with interaction between the fixed factors. To proceed with the analysis, we used a model with a compound symmetry structure. One-way ANOVA was performed to analyze fasting plasma values in the subject groups. For most variables, values were log-transformed to stabilize variances. Reported *P* values are based on these transformations. The univariate normality assumptions were verified with the Shapiro-Wilk test. The Brown and Forsythe variation of Levene's test statistic was used to verify the homogeneity of variances. Relationships between variables were expressed using Pearson correlation coefficients, and linear regression analyses were performed for comparisons between regression lines. For multiple regression analysis, a stepwise forward model was used. The results were considered significant at $P \leq 0.05$, with a power of $\alpha = 0.05$. Statistical analyses were conducted using the statistical package SAS, version 9.1.3 (SAS Institute, Inc., Cary, NC). Graphical analyses were done using GraphPad Prism (San Diego, CA).

RESULTS

Subject characteristics

A total of 16 subjects participated in this study. A fasting blood sample and adipose tissue SC and OM samples were taken from each subject. Of the 28 adipose samples, 24 were paired OM and SC samples from 12 subjects, and the remaining 4 samples were unpaired. As shown in **Table 1**, the subjects were divided into two groups, NO (n = 5) and obese (n = 11), based on body mass index (BMI), where a BMI > 30 kg/m^2 is considered obese. Furthermore, the obese subjects were selected based on relative insulin sensitivity into "relatively ISO" and "relatively IRO" groups, based on fasting insulin levels (where "insulin resistant" > 400 pmol/l), resulting in three groups: NO (BMI = 26.3 ± 1.0 kg/m^2, insulin = 146.4 ± 23.7 pmol/l); ISO (BMI = 47.4 ± 3.5 kg/m^2, insulin = 260.1 ± 33.3 pmol/l); and IRO (BMI = 60.9 ± 4.2 kg/m^2, insulin = 507.4 ± 32.5 pmol/l). Note that, overall, ISO subjects constitute a small proportion of obese subjects (29). There was no significant difference in insulin levels between the ISO and NO groups, although IRO levels were increased significantly (Table 1). There was no significant difference in BMI in the IRO group compared with the ISO group, and both groups would be considered morbidly obese (BMI > 40 kg/m^2) (30).

As shown in Table 1, both the NO and ISO groups had normal glucose levels that were not significantly different from each other (fasting plasma glucose < 6.0 mmol/l; NS), whereas the IRO group had significantly increased glucose levels (fasting glucose > 7.0 mmol/l; $P < 0.05$), comparable to levels in insulin resistance (31), although none had been diagnosed as diabetic. There was no significant difference in age among the three groups, nor was there a difference in gender distribution for any of the variables (by Chi-square analysis). Furthermore, for all of the ANOVA analyses described below, inclusion of gender (two-way ANOVA) had no effect on the statistical outcome. Age did not correlate with HOMA-IR, BMI, or circulating insulin levels (NS for all).

Microarray analysis

To avoid bias based on selecting only a few samples from the group for microarray analysis, all 28 samples were analyzed. A number of different analysis paradigms were used for the initial evaluation of the microarray results. As the primary hypothesis was to evaluate the more IRO subjects (n = 6) versus the relatively ISO and lean subjects (ISO+NO; n = 10), we first compared these two groups.

TABLE 1. Subject characteristics

Variable	Group			*P*
	NO	ISO	IRO	
Number	5	5	6	
Female/male	3/2	4/1	5/1	NS
Age	52.6 ± 6.3 (34–64)	39.8 ± 5.6 (29–54)	44.4 ± 2.5 (37–52)	NS
BMI	25.1 ± 1.4 (20.4–28.4)	47.4 ± 3.5[a] (40–58)	60.9 ± 5.6[b] (43–63)	<0.0001
Glucose	3.81 ± 0.17 (3.20–4.19)	5.41 ± 1.15 (3.50–9.85)	7.05 ± 1.28[c] (4.34–12.08)	0.02
Insulin	152 ± 19 (106–208)	260 ± 33 (163–346)	507 ± 36[b,d] (422–638)	<0.0001
HOMA-IR	3.68 ± 0.48 (2.51–5.43)	9.36 ± 2.84 (4.82–20.35)	24.42 ± 5.27[a] (11.86–32.81)	0.04
Triglyceride	1.21 ± 0.16 (0.72–1.57)	1.74 ± 0.14 (1.50–2.29)	1.73 ± 0.37 (1.02–3.28)	NS
NEFA	0.162 ± 0.074 (0.066–0.457)	0.231 ± 0.059 (0.082–0.439)	0.350 ± 0.06 (0.214–0.578)	NS
Total cholesterol	4.48 ± 0.75 (2.83–6.91)	4.81 ± 0.16 (4.35–5.31)	4.37 ± 0.44 (3.42–5.69)	NS
LDL cholesterol	2.70 ± 0.064 (1.22–4.55)	3.11 ± 0.09 (2.83–3.29)	2.06 ± 0.18 (1.64–3.45)	NS
HDL cholesterol	1.23 ± 0.21 (0.87–2.03)	0.99 ± 0.02 (0.92–1.03)	1.20 ± 0.08 (0.89–1.33)	NS

HOMA-IR, homeostasis model assessment insulin resistance; IRO, insulin-resistant obese; ISO, insulin-sensitive obese; NO, nonobese. Age (years), body mass index (BMI; kg/m^2), fasting plasma insulin levels (pmol/l), fasting plasma glucose levels (mmol/l), HOMA-IR index, and plasma lipids (triglyceride, total cholesterol, LDL cholesterol, and HDL cholesterol, all in mmol/l) for NO (n = 5), ISO (n = 5), and IRO (n = 6) subjects are presented as means ± SEM (with minimum to maximum range indicated for each variable in parentheses).

[a] $P < 0.01$ versus NO.

[b] $P < 0.001$ versus NO.

[c] $P < 0.05$ versus NO.

[d] $P < 0.001$, IRO versus ISO.

Because the ISO and NO groups were not significantly different based on either fasting glucose or insulin level, and no major gene differences were identified between these two groups in the majority of analyses (except where noted), these two groups were pooled (ISO+NO). The cDNA microarrays contained a total of ~20,000 probes (~10,000 human genes, plus expressed sequence tags, housekeeping genes, and positive and negative controls), which were analyzed for 28 samples altogether. Specific information on Codelink Uniset 20K I Gene List 30019 can be obtained directly (www.gehealthcare.com/usen/microarrays/codelink_genelists.html). The complete data set will be reported in GEO (for Gene Expression Omnibus), available at www.ncbi.nlm.nih.gov/geo/.

SAM analysis was performed on SC and OM samples separately using the same analysis parameters. With an estimated FDR of 0.5% and a minimum 3-fold change, 941 genes were identified as significantly different in OM tissue comparing IRO and ISO+NO. Using the same analysis parameters, no genes were identified as significantly different in SC tissue comparing IRO and ISO+NO. Using less stringent criteria (FDR = 15% and minimum 3-fold change), 534 genes were identified. When gene expression in OM tissue was compared directly with that in SC tissue, using paired analysis and the stringent parameters (0.5% FDR and minimum 3-fold difference), no genes were identified. Using less stringent criteria (FDR = 5% and minimum 2-fold change), only 48 significant genes were identified. Therefore, by far, the major differences in gene expression in this sample set appear to be the differences related to insulin sensitivity in OM tissue (IRO vs. ISO+NO).

The genes identified in OM adipose tissue were further examined. Of those representing identified genes, 482 were upregulated (positive genes) and 312 were downregulated (negative genes) in IRO subjects compared with ISO+NO subjects. Gene description and access to Codelink Uniset 20K I Gene List 30019 (www.gehealthcare.com/usen/microarrays/codelink_genelists.html) were used to assign the regulated genes into functional categories. Of the genes with assigned function, positively regulated genes coded for proteins involved in extracellular signaling (including cell-cell signaling and endocrine functions; 24%), intracellular signaling (12%), intermediary metabolism and energy metabolism (8%), structural proteins (6%), and transcription and translation (including cell growth, differentiation, apoptosis, and proteolysis; 40%). For negatively regulated genes, these same distributions were 6, 9, 17, 2, and 40%, respectively. Supplementary tables listing the positive and negative genes are included (see supplementary Tables I and II).

Analysis based on insulin sensitivity versus obesity

Specific analysis of genes of interest was then undertaken, including, first, housekeeping genes (as controls), then insulin signaling pathway genes, including InsR, IRS-1, and positive and negative regulators, as well as the well-defined insulin pathways of glucose metabolism, transcriptional and translational regulation of protein synthesis, proliferation, and differentiation in both OM and SC tissues. Using this direct approach of analysis of the specific insulin signaling pathways (excluding the housekeeping genes), of the 47 specific genes identified, 34 (72%) demonstrated significant changes related to insulin sensitivity (**Table 2**), either increased or decreased. This is a significant enrichment ($P < 0.001$ by Chi-square analysis) compared with the general nontargeted approach using SAM, which identified 941 genes of 20,000 (4.7%). Analysis by two-way ANOVA, taking into account both groups (IRO vs. ISO+NO) and tissues (SC vs. OM), indicated that there was no overall significant tissue difference (Table 2). Nonetheless, using the targeted analysis of insulin signaling pathway genes, the changes were more pronounced in the OM adipose tissue than in the SC (on average, 30% greater; Table 2), in agreement with the SAM analysis.

Furthermore, to identify differences that could be attributed specifically to obesity (or BMI) rather than to insulin sensitivity (based on plasma insulin values), we also compared NO and obese subjects (ISO+IRO). Overall, based on group analysis, only two genes, IKK and SHC, were found to be significantly different (both $P = 0.02$). Furthermore, Pearson analysis indicated that only five genes (PDK4, IKK, Rheb, SHC, and PPARα) correlated with BMI (Table 2), two of which (PDK4 and PPARα) had no correlation with insulin sensitivity (as determined by correlation to InsR or plasma insulin values or by two-way ANOVA; Table 2). Further comments are provided below for IKK, Rheb, and SHC.

Housekeeping genes

The expression of four housekeeping genes (32) across all 28 samples was evaluated (**Table 3**). The expression of HPRT1, TFRC, B2M, and PPIA was constant across all 28 samples. There were no significant correlations between any of the housekeeping genes and age, BMI, or fasting insulin. When separated into three groups (NO, ISO, and IRO) and two tissues (OM and SC), analysis failed to reveal significant differences in expression of the five housekeeping genes. Furthermore, the expression of constant levels of B2M was confirmed using real-time PCR on all 28 samples individually (Table 3).

InsR and IRS-1 mRNA

InsR and IRS-1 are two key signaling proteins common to all of the insulin signaling pathways (26). Comparison between IRO and ISO+NO overall indicated a group difference based on insulin sensitivity (Table 2). In the OM tissue, expression of InsR in the IRO group was significantly higher than in both the ISO group ($P = 0.01$) and the NO insulin-sensitive group ($P = 0.01$; **Fig. 1A**). The same pattern emerged for the expression of IRS-1. In OM tissue, expression in the IRO group was substantially higher than in either of the two insulin-sensitive groups (Fig. 1B). When NO and ISO data were pooled, the OM insulin-sensitive groups were significantly lower than the IRO group (Table 2). On the other hand, in SC tissue, whereas the IRO group was greater than the pooled ISO+NO group (Table 2), examination of the ISO and NO groups individually (Fig. 1A, B) demonstrated that they were not comparable. For all of the genes examined, this was the case

TABLE 2. Comprehensive list of insulin signaling genes analyzed by microarray

Gene	Accession Number	SC Adipose Tissue NO	SC Adipose Tissue ISO	SC Adipose Tissue IRO	SC Adipose Tissue IRO/NO+ISO	OM Adipose Tissue NO	OM Adipose Tissue ISO	OM Adipose Tissue IRO	OM Adipose Tissue IRO/NO+ISO	*P*	Pearson Correlation InsR	Pearson Correlation Plasma Insulin	Pearson Correlation BMI
InsR	X02160	14.515 ± 5.518	4.721 ± 1.184	11.903 ± 3.891	131%	2.776 ± 0.819	6.134 ± 2.032	17.666 ± 2.931	362%	0.005		0.385[a]	0.280
IRS-1	NM_005544	7.190 ± 2.107	3.950 ± 0.906	6.795 ± 1.929	126%	1.353 ± 0.466	4.396 ± 1.194	7.709 ± 1.103	237%	0.033	0.881[b]	0.334	0.302
IRS-4	NM_003604	3.316 ± 0.794	2.627 ± 0.684	4.561 ± 1.137	156%	3.546 ± 1.630	2.149 ± 0.245	4.487 ± 0.758	168%	0.033	0.514[c]	0.455[a]	0.294
Glucose transport pathway													
PI3K p110 γ	NM_002649	0.752 ± 0.099	0.805 ± 0.192	0.921 ± 0.074	118%	0.496 ± 0.027	0.615 ± 0.070	0.859 ± 0.154	151%	0.009	0.505[c]	0.302	0.252
PI3K p110α	NM_006218	1.043 ± 0.429	1.657 ± 0.369	0.684 ± 0.274	49%	1.672 ± 0.241	1.717 ± 0.482	0.809 ± 0.179	48%	0.020	−0.705[b]	−0.350	−0.120
P13K p110β	NM_006219	0.456 ± 0.215	0.460 ± 0.138	0.345 ± 0.073	75%	0.641 ± 0.163	0.591 ± 0.087	0.426 ± 0.083	70%	NS	−0.418[a]	−0.232	−0.072
PDK1	NM_002610	0.271 ± 0.074	0.304 ± 0.064	0.147 ± 0.061	51%	0.479 ± 0.063	0.239 ± 0.024	0.413 ± 0.178	125%	NS	−0.155	0.020	0.066
PDK2	NM_002611	1.952 ± 1.013	3.078 ± 0.895	0.993 ± 0.399	39%	2.487 ± 0.406	2.451 ± 0.196	0.957 ± 0.249	39%	0.010	−0.619[b]	−0.547[c]	−0.315
PDK3	NM_005391	0.261 ± 0.050	0.322 ± 0.054	0.303 ± 0.097	103%	0.465 ± 0.231	0.308 ± 0.040	0.316 ± 0.053	86%	NS	−0.320	−0.105	−0.043
PDK4	NM_002612	0.311 ± 0.138	0.347 ± 0.135	0.328 ± 0.104	99%	0.267 ± 0.088	0.402 ± 0.128	0.532 ± 0.176	151%	NS	0.011	0.296	0.478[c]
Akt2	NM_001626	0.262 ± 0.073	0.218 ± 0.029	0.613 ± 0.305	258%	0.289 ± 0.114	0.165 ± 0.055	0.337 ± 0.091	160%	0.023	0.186	0.370	0.056
PKBγ	NM_005465	0.118 ± 0.060	0.230 ± 0.064	0.163 ± 0.045	88%	0.144 ± 0.091	0.182 ± 0.061	0.306 ± 0.125	183%	NS	0.340	0.187	0.254
GSK-3β	NM_002093	4.564 ± 0.459	3.196 ± 0.478	4.755 ± 1.211	125%	3.636 ± 0.203	2.985 ± 0.372	3.929 ± 0.521	122%	NS	0.603[b]	0.070	0.119
GLUT4	NM_006516	0.234 ± 0.052	0.231 ± 0.079	0.499 ± 0.165	214%	0.198 ± 0.021	0.147 ± 0.030	0.499 ± 0.113	300%	0.050	0.326	0.559[c]	0.360
GLUT1	NM_001042	0.157 ± 0.037	0.157 ± 0.052	0.273 ± 0.156	174%	0.194 ± 0.058	0.097 ± 0.039	0.226 ± 0.173	169%	0.003	0.285	0.134	−0.001
Regulators of InsR and IRS-1													
SOCS	NM_003955	0.473 ± 0.216	0.502 ± 0.234	0.315 ± 0.069	64%	0.233 ± 0.027	0.172 ± 0.082	0.258 ± 0.084	132%	NS	0.002	−0.197	−0.171
PTP1B	NM_002827	1.181 ± 0.185	0.916 ± 0.103	1.613 ± 0.368	156%	1.272 ± 0.319	0.945 ± 0.113	1.179 ± 0.159	110%	NS	0.499[c]	0.213	0.241
Jnk	NM_002750	0.113 ± 0.042	0.080 ± 0.040	0.246 ± 0.086	240%	0.102 ± 0.032	0.106 ± 0.033	0.310 ± 0.105	290%	0.010	0.410[a]	0.400[a]	0.316
IKK	NM_001278	0.231 ± 0.013	0.147 ± 0.038	0.500 ± 0.173	272%	0.096 ± 0.048	0.242 ± 0.068	0.472 ± 0.126	363%	0.001	0.382[a]	0.538[c]	0.395[a]
Rheb	NM_005614	16.88 ± 3.530	20.24 ± 3.041	10.516 ± 3.260	56%	20.579 ± 1.930	18.131 ± 2.083	8.057 ± 2.774	42%	0.001	−0.697[b]	−0.572[c]	−0.381[a]
mTor	NM_004958	0.653 ± 0.345	1.240 ± 0.318	0.695 ± 0.269	71%	1.416 ± 0.352	1.008 ± 0.245	0.539 ± 0.166	46%	0.050	−0.664[b]	−0.259	−0.133
S6K	NM_003161	0.415 ± 0.043	0.317 ± 0.044	0.572 ± 0.216	159%	0.233 ± 0.078	0.271 ± 0.050	0.317 ± 0.096	124%	0.023	0.172	0.252	0.028
Protein synthesis pathway													
eIF4E	NM_001968	0.919 ± 0.534	1.219 ± 0.352	0.621 ± 0.275	57%	1.521 ± 0.506	1.540 ± 0.657	0.410 ± 0.125	27%	0.026	−0.565[c]	−0.265	−0.103
eIF4A1	NM_001416	3.037 ± 1.734	6.431 ± 1.717	2.511 ± 1.811	51%	4.522 ± 3.491	6.098 ± 1.398	1.427 ± 0.686	22%	0.014	−0.694[b]	−0.353	−0.183
eIF4A2	NM_001967	3.598 ± 3.134	6.241 ± 2.208	2.753 ± 2.355	54%	9.959 ± 3.891	9.147 ± 3.170	1.223 ± 0.634	13%	0.020	−0.681[b]	−0.360	−0.200
eIF4G1	NM_001417	11.35 ± 2.337	16.380 ± 3.765	9.908 ± 2.396	70%	10.790 ± 0.467	12.880 ± 1.871	10.550 ± 1.563	87%	0.020	−0.331	−0.208	0.075
eIF4G2	NM_001418	2.123 ± 1.899	4.871 ± 2.042	1.463 ± 0.936	40%	7.030 ± 2.433	5.058 ± 2.041	0.605 ± 0.089	10%	0.045	−0.628[b]	−0.352	−0.187
eIF4G3	NM_003760	2.755 ± 0.488	2.522 ± 0.444	1.857 ± 0.507	71%	2.795 ± 0.081	3.831 ± 0.676	2.765 ± 0.665	80%	0.008	−0.233	−0.169	−0.127
4EBP1	NM_004095	4.007 ± 1.561	4.106 ± 1.319	2.393 ± 0.768	59%	5.297 ± 0.966	4.615 ± 0.945	2.875 ± 0.649	59%	0.030	−0.404[a]	−0.391[a]	−0.285
4EBP2	NM_004096	9.902 ± 1.803	12.520 ± 1.793	8.443 ± 1.160	74%	17.95 ± 6.122	11.050 ± 3.131	6.006 ± 0.895	44%	0.032	−0.435[a]	−0.488[c]	−0.342
4EBP3	NM_003732	1.795 ± 0.323	2.221 ± 0.439	1.759 ± 0.581	87%	2.208 ± 0.258	1.806 ± 0.190	1.527 ± 0.370	78%	NS	−0.544[c]	−0.198	−0.043
Proliferation pathway													
SHC	NM_016848	0.241 ± 0.059	0.267 ± 0.075	0.487 ± 0.121	191%	0.190 ± 0.035	0.225 ± 0.040	0.588 ± 0.152	277%	0.010	0.480[c]	0.566[c]	0.482[c]
GRB2	NM_002086	0.701 ± 0.047	0.680 ± 0.078	0.784 ± 0.199	114%	0.629 ± 0.081	0.738 ± 0.094	0.866 ± 0.064	124%	NS	0.399[a]	0.105	0.287
SOS	NM_005633	1.549 ± 0.237	1.654 ± 0.363	2.262 ± 0.576	141%	1.305 ± 0.208	1.241 ± 0.150	1.969 ± 0.221	156%	0.022	0.423[a]	0.386[a]	0.167
Ras	NM_005343	2.196 ± 0.723	3.026 ± 0.474	1.984 ± 0.734	75%	2.775 ± 0.657	2.582 ± 0.377	2.115 ± 0.632	80%	0.023	−0.381[a]	−0.090	−0.023
Raf-1	NM_002880	2.002 ± 0.415	1.784 ± 0.483	2.212 ± 0.302	118%	1.199 ± 0.157	1.434 ± 0.140	2.133 ± 0.297	158%	0.038	0.725[b]	0.309	0.266
MEK1/2 kinase 1	NM_002755	2.158 ± 1.072	3.809 ± 1.091	1.575 ± 0.844	51%	3.657 ± 0.555	2.727 ± 0.593	0.976 ± 0.117	32%	0.009	−0.644[b]	−0.370	−0.186
MEK1/2 kinase 2	NM_030662	0.520 ± 0.156	0.765 ± 0.182	0.522 ± 0.196	80%	0.684 ± 0.143	0.684 ± 0.074	0.493 ± 0.100	72%	NS	−0.323	−0.273	−0.046
Differentiation pathway													
PPARα	NM_005036	0.918 ± 0.165	0.624 ± 0.036	0.719 ± 0.104	95%	0.937 ± 0.318	0.509 ± 0.030	0.459 ± 0.130	69%	NS	−0.0836	−0.363	−0.453[a]
PPARγ	NM_005037	11.767 ± 4.659	16.610 ± 4.457	6.868 ± 1.828	47%	15.511 ± 6.460	11.269 ± 2.672	4.580 ± 1.144	36%	0.014	−0.619[b]	−0.510[c]	−0.287
PPARδ	NM_006238	0.609 ± 0.106	0.572 ± 0.106	0.865 ± 0.280	147%	0.419 ± 0.075	0.418 ± 0.030	0.801 ± 0.173	191%	0.034	0.434[a]	0.361	0.150
PPARγ coactivator 1	NM_013261	0.266 ± 0.076	0.184 ± 0.035	0.421 ± 0.264	191%	0.080 ± 0.039	0.117 ± 0.023	0.371 ± 0.097	359%	0.028	0.325	0.437[a]	0.140
CEBPϵ	NM_001805	0.146 ± 0.049	0.180 ± 0.070	0.263 ± 0.051	158%	0.208 ± 0.032	0.074 ± 0.035	0.388 ± 0.111	311%	0.001	0.455[a]	0.491[c]	0.353
CEBPγ	NM_001806	22.053 ± 7.941	9.479 ± 0.253	18.752 ± 5.025	124%	8.779 ± 2.174	9.289 ± 1.767	18.170 ± 1.621	200%	0.020	0.878[b]	0.236	0.138
CEBPα	NM_004364	21.020 ± 8.722	32.894 ± 6.472	12.107 ± 4.255	44%	27.740 ± 9.498	17.788 ± 3.157	9.857 ± 3.440	46%	0.002	−0.599[b]	−0.460[a]	−0.276
CEBPβ	NM_005194	2.014 ± 1.651	2.389 ± 1.184	1.130 ± 0.692	51%	1.818 ± 0.066	1.968 ± 0.535	0.768 ± 0.207	40%	0.050	−0.527[c]	−0.341	−0.209
CEBPδ	NM_005195	0.374 ± 0.206	0.595 ± 0.308	0.406 ± 0.084	82%	0.262 ± 0.060	0.450 ± 0.115	0.594 ± 0.181	157%	NS	−0.0331	0.064	0.204

InsR, insulin receptor; IRS-1, insulin receptor substrate 1. Data presented are gene expression analysis of SC and OM adipose tissue from NO (n = 3–4), ISO (n = 5), and IRO (n = 5–6) groups analyzed by microarray. The associated accession numbers are reported. Means and SEM are presented for each group (all units are arbitrary), and percentage change IRO/NO+ISO is given for SC and OM tissues separately. Two-way paired ANOVA (group and tissue) analysis was performed on the SC and the OM groups, with *P* values reported for group significance (IRO vs. NO+ISO). In all cases, there was no significant tissue difference and no group×tissue interaction. Pearson correlations (*r* values) between each gene and InsR expression, plasma insulin values, and BMI are provided, where significance was set at $P < 0.05$.

[a] $P < 0.05$.
[b] $P < 0.001$.
[c] $P < 0.01$.

TABLE 3. Endogenous controls

Group	HPRT1	TFRC	PPIA	B2M	B2M Real-Time PCR
SC					
NO	0.778 ± 0.068	0.283 ± 0.073	21.4 ± 3.6	128.8 ± 9.3	1.28 ± 0.37
ISO	0.829 ± 0.208	0.186 ± 0.044	25.0 ± 3.6	115.6 ± 17.1	4.09 ± 2.18
IRO	0.517 ± 0.204	0.247 ± 0.046	18.7 ± 5.5	124.7 ± 31.2	5.03 ± 2.33
P	NS	NS	NS	NS	NS
OM					
NO	0.910 ± 0.485	0.276 ± 0.119	22.2 ± 5.8	123.2 ± 16.8	1.48 ± 0.74
ISO	0.720 ± 0.145	0.243 ± 0.042	24.8 ± 3.5	118.0 ± 13.0	0.52 ± 0.27
IRO	0.558 ± 0.145	0.372 ± 0.104	17.5 ± 5.2	83.9 ± 18.9	2.24 ± 1.43
P	NS	NS	NS	NS	NS

Mean microarray values ± SEM for subcutaneous (SC) and omental (OM) tissues in NO, ISO, and IRO groups assessed by CodeLink microarray for four endogenous controls: HPRT1 (accession number NM_000194), TFRC (NM_003234), PPIA (NM_021130), and B2M (NM_004048). Confirmation of B2M gene expression was performed using real-time TAQMAN PCR for all samples individually. Significance was set at $P < 0.05$, where NS indicates not significant. All units are arbitrary.

only for InsR and IRS-1. Results for IRS-1 were also confirmed by real-time PCR for all 28 samples individually (Fig. 1B, inset). Regardless of insulin status and body size, these two genes correlated very strongly ($r = 0.881$, $P < 0.0001$; Fig. 1C), despite neither of them correlating with BMI (Table 2) or age (NS). Note that InsR and IRS-1 individually correlated significantly in OM tissue alone and SC tissue alone, with no significant difference between the linear regressions; hence, pooled analysis is presented. Furthermore, InsR correlated positively with fasting insulin levels ($r = 0.385$, $P < 0.05$; Table 2). IRS-4 expression was also significantly altered in the three groups (Table 2; $P = 0.033$), demonstrating consistency within the pathway.

Glucose transport pathway

The glucose transport pathway of insulin signaling includes PI3K, PDK1/2, Akt, GSK-3βBβ, and GLUT4 proteins (26, 33). Results for these genes are given in Table 2 (SC and OM) and **Fig. 2**. Several important changes in gene expression of the glucose pathway were identified. By two-way paired ANOVA analysis, significant differences were seen in the IRO group compared with the ISO+NO group for PI3Kα, PI3Kγ, PDK2, Akt2, GLUT4, and GLUT1 (Table 2). There were no differences between ISO and NO expression; thus, the data for these two groups were pooled for analysis. Furthermore, there were no tissue (OM vs. SC) differences and no group×tissue interaction. In each case, group differences were based on insulin sensitivity status rather than obesity (BMI) (Table 2). Examples of individual results are shown for OM tissue in Fig. 2A–C. PI3Kα and PDK2 expression were significantly lower in the IRO group (Fig. 2A, B; $P < 0.05$, $P < 0.01$, respectively). The expression pattern of PDK2 was confirmed using real-time PCR in all 28 samples (for OM, Fig. 2B, inset; data not shown for SC). GLUT4 was also altered in the IRO group but demonstrated the opposite pattern of expression with higher expression in the IRO group ($P < 0.05$; Fig. 2C). PI3Kγ, Akt2, and GLUT1 expression also increased overall (all $P < 0.05$; Table 2).

Within the families of genes that were examined (PI3K and PDK), specificity is demonstrated by alterations in the expression of select isoforms in each case. The β isoform of the PI3K family was unchanged, whereas PI3Kα and PI3Kγ were changed. Within the PDK family, a similar trend of specificity was observed; only PDK2, but not PDK1, PDK3, or PDK4, had altered expression in the IRO group (Table 2). The specificity in gene regulation within the pathway was also related to the signaling pathway in this case; neither PKBγ nor GSK-3β genes were altered (Table 2).

There are several strong correlations both within the glucose transport pathway and between these genes and InsR and IRS-1 in adipose tissue. Figure 2F shows the strong negative correlation between PDK2 and InsR, but equally striking correlations between PI3Kα, PI3Kγ, and GLUT4 also exist (**Table 4**). Within the group, the correlation between PDK2 and PI3Kα (Fig. 2D) and between GLUT4 and PI3Kγ ($r = 0.676$, $P < 0.01$) were strongly positive, whereas the correlation between GLUT4 and PDK2 (Fig. 2E) was negative ($r = -0.762$, $P < 0.01$). In each case, both the SC and OM were significant individually, and the regression was not different from each other. However, because of the pronounced changes in OM tissue, correlations for OM tissue alone were generally stronger. Additional correlations between genes in the glucose transport pathway are given in Table 4. Furthermore, fasting insulin levels correlated negatively with PDK2 ($r = -0.547$, $P < 0.01$; Table 2) and positively with GLUT4 ($r = 0.559$, $P < 0.01$). None of the glucose pathway gene expressions correlated with age using all data points (SC+OM) or OM only gene expression (NS).

Regulators of InsR and IRS-1

InsR and IRS-1 are themselves regulated by several intracellular proteins. Four genes of particular note are SOCS and PTP-1B, which negatively regulate InsR, and Jnk and IKK, which negatively regulate IRS-1 (34, 25). In the present study, these genes were expressed at similar levels between SC and OM tissue (NS), with the exception of IKK, which was expressed at a lower level in OM tissue ($P < 0.05$; **Fig. 3B**). As shown in Table 2, whereas SOCS and PTP-1B showed no significant change, both IKK and Jnk were significantly different by group based on two-way paired ANOVA analysis, as also shown in Fig. 3A, B. This pattern of increased IKK expression in the IRO group was confirmed using real-time PCR in both

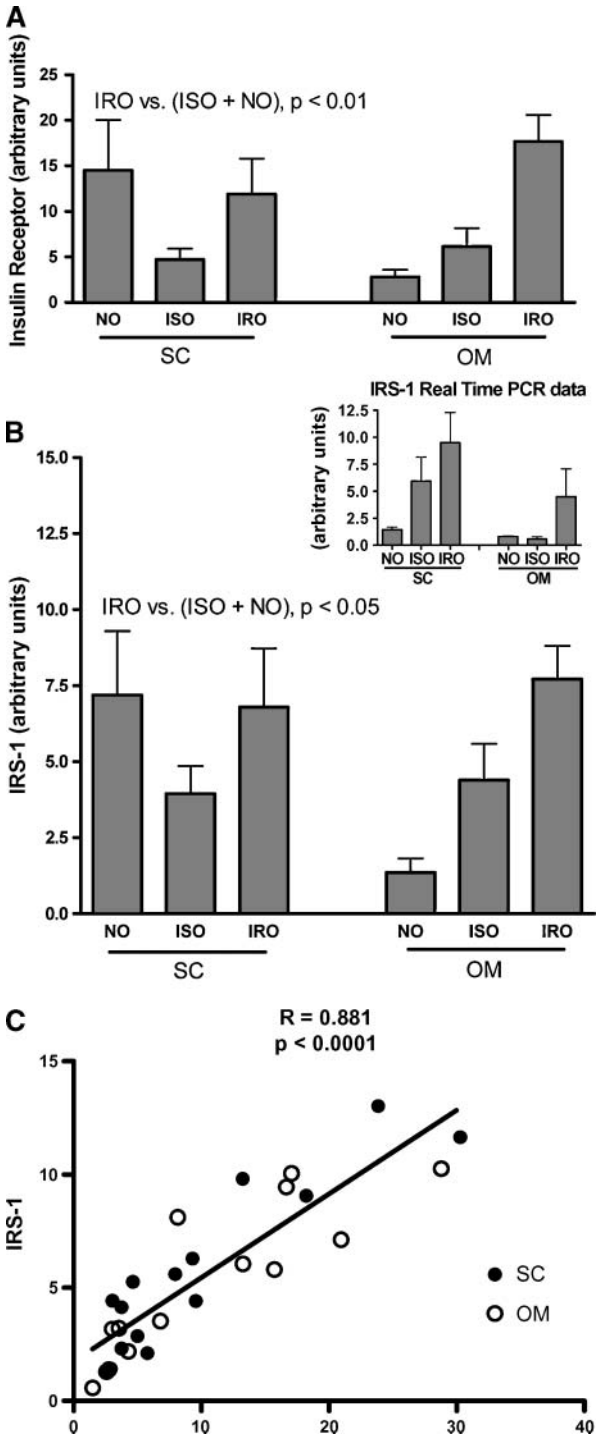

Fig. 1. Insulin receptor (InsR) and insulin receptor substrate 1 (IRS-1) follow similar patterns of gene expression. A, B: Gene expression of InsR (A) and IRS-1 (B) in subcutaneous (SC) and omental (OM) human adipose tissue from nonobese (NO; n = 3–4), insulin-sensitive obese (ISO; n = 5), and insulin-resistant obese (IRO; n = 5–6) subjects as assessed by CodeLink microarray. Confirmation of IRS-1 gene expression by real-time TAQMAN PCR is shown in the inset in B. Data shown are means ± SEM. C: Correlation between InsR and IRS-1 in both SC (closed circles) and OM (open circles) pooled samples. Individual correlations in SC only and in OM only were both significant ($P < 0.0001$), and regression lines were not significantly different from each other.

SC and OM tissue (Fig. 3B, inset). Furthermore, the expression of IKK and Jnk correlated strongly with each other (Fig. 3C), and each correlated with InsR (Fig. 3D, Table 2) as well as with plasma insulin (Table 2). None of these regulated genes correlated with age. Most (11 of 13) of the genes that correlated with plasma insulin also correlated with InsR. Indeed, the majority (31) of the genes examined in Table 2 correlated with InsR; however, only 5 correlated with BMI. Very few (three) correlated with both. IKK was one of these three genes. Note, however, that whereas IKK correlated individually with InsR, plasma insulin, and BMI (Table 2; Pearson correlation), in multiple regression analysis, in spite of forced entry of BMI into the equation, plasma insulin contributed significantly ($P = 0.03$) to predicting IKK ($r = 0.541$), whereas BMI did not contribute additionally ($P = 0.755$).

mTor, S6K, and Rheb as negative regulators of IRS-1

PI3K, Akt, and Rheb are activators of mTor (35). mTor and its effector S6K can act as negative regulators of IRS-1 (36). Gene expression of all three of these proteins was the same in SC and OM tissue of NO subjects (NS). As analyzed by two-way paired ANOVA, Rheb ($P = 0.001$) and mTor ($P = 0.05$) demonstrated significant group effects, with a pronounced decrease in the IRO group (Table 2). **Figure 4A** shows that mTor expression levels in IRO OM tissue were lower ($P < 0.05$); the expression pattern of mTor was confirmed by real-time PCR for all 28 samples in both SC (data not shown) and OM tissue (Fig. 4A, inset).

The consistency of this pattern led to a strong positive correlation between mTor and Rheb (Fig. 4E). Furthermore, both Rheb (Fig. 4D) and mTor ($r = -0.664$, $P < 0.001$) had strong negative correlations with InsR (Table 2) as well as with IRS-1 ($r = -0.764$, $P = 0.001$ and $r = -0.801$, $P < 0.001$, respectively). By contrast, S6K demonstrated a slight (but significant) increase in IRO ($P = 0.023$, two-way paired ANOVA; Table 2), although correlations with InsR (Table 2) and IRS-1 were not significant. However, S6K did correlate positively with Jnk and IKK (other negative regulators of IRS-1; **Table 5**), whereas Rheb correlated negatively with these genes. Within the Rheb/mTor/S6K pathway, age did not correlate with any of the genes (NS), whereas Rheb correlated with both insulin and BMI (Table 2). Note that, in multiple regression analysis, in spite of forced entry of BMI into the equation, Rheb was best predicted with a linear combination ($r = 0.777$) of InsR ($P < 0.001$) and insulin ($P = 0.03$), whereas BMI did not contribute significantly ($P = 0.461$).

mTOR, S6K, 4EBP, and eIF protein synthesis

mTor and S6K play dual roles in insulin signaling physiology. Both insulin and nutrient status can lead to mTor activation that ultimately increases protein synthesis via enhanced translation (25). Key players in this pathway include Raptor, S6K1, S6, the 4EBP family (4EBP1, 4EBP2, and 4EBP3), and the eIF family (eIF4A, eIF4G, and eIF4E) (37). Consistent with the other pathways examined, the

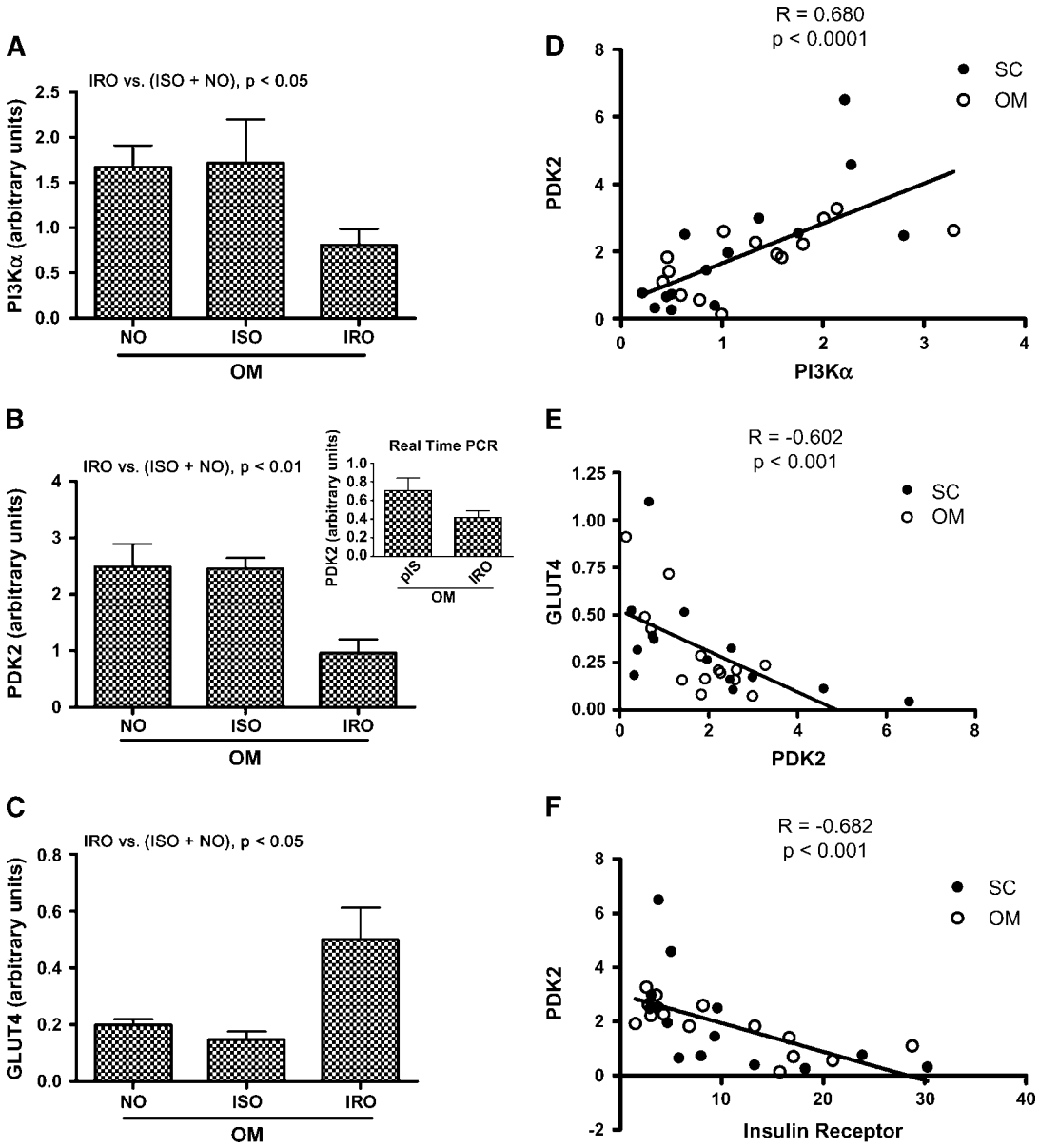

Fig. 2. In the glucose pathway, PI3Kα, PDK2, and GLUT4 are altered in IRO subjects. A–C: Gene expression of PI3Kα (A), PDK2 (B), and GLUT4 (C) in OM human adipose tissue from NO (n = 3), ISO (n = 5), and IRO (n = 6) subjects as assessed by CodeLink microarray. Confirmation of PDK2 gene expression by real-time TAQMAN PCR is shown in the inset in B. pIS, pooled insulin sensitive (NO + ISO). Data shown are means ± SEM. C–F: Correlation between PDK2 and PI3Kα (D), PDK2 and GLUT4 (E), and PDK2 and InsR (F) pooled for SC (closed circles) and OM (open circles) samples. Individual correlations in SC only and in OM only were all significant ($P = 0.02$ to $P < 0.001$), and SC and OM regression lines were not significantly different from each other in all cases.

basal expression in the NO group was not different between SC and OM tissues.

The altered pattern of expression in the IRO group in the eIF family was particularly striking. In each case, there was a marked decrease in expression in IRO groups across both OM and SC tissue (Table 2; all six isoforms were significantly decreased by two-way paired ANOVA, with greater percentage changes in OM). An example of one gene, eIF4A2, is shown in Fig. 4B. Furthermore, of the three 4EBP genes, 4EBP1 (Fig. 4C) and 4EBP2 demonstrated a similar trend of lower expression in the IRO group ($P < 0.05$ for both by two-way ANOVA; Table 2), whereas 4EBP3 was not altered. In fact, of all the genes examined in the protein synthesis pathway, all except S6K were decreased in IRO subjects.

The consistency of this pattern is highlighted by the strong correlations between the genes, which may be a reflection of the gene synergy. Within the protein translation genes, the tight correlation between eIF4A2 and eIF4G2 is shown in Fig. 4F; however, several other strong correlations exist, including strong correlations between Rheb/mTor and the eIF family (shown for OM tissue in **Table 6**). Between the genes involved in protein transla-

TABLE 4. Pearson correlations within the glucose pathway

	PI3Kα	PI3Kβ	PDK1	PDK2	PDK3	PDK4	Akt2	PKBγ	GSK3β	GLUT4	GLUT1
PI3Kγ	−0.374	0.223	0.323	−0.455	−0.147	0.507	0.424	0.780[a]	0.030	0.676[b]	0.326
PI3Kα		0.647[c]	0.005	0.661[b]	0.180	0.125	−0.619[c]	−0.130	−0.606[c]	−0.338	−0.317
PI3Kβ			0.374	0.509	0.188	0.348	−0.228	0.309	−0.536[c]	0.047	−0.083
PDK1				−0.290	0.159	0.641[c]	0.312	−0.010	−0.507	0.603[c]	−0.542[c]
PDK2					−0.091	−0.369	−0.628[c]	−0.268	−0.370	−0.762[b]	−0.061
PDK3						−0.150	0.350	0.092	−0.122	0.023	0.153
PDK4							0.126	0.273	−0.362	0.740[b]	−0.319
Akt2								0.199	0.361	0.450	0.232
PKBγ									0.183	0.411	0.627[c]
GSK-3β										0.059	0.634[c]
GLUT4											0.011

[a] $P < 0.001$.
[b] $P < 0.01$.
[c] $P < 0.05$.

tion and both InsR and IRS-1, there were other correlations as well. Of note, in the eIF family, most isoforms that were altered in the IRO group correlated with both InsR (Table 2) and IRS-1 (data not shown). 4EBP1, 4EBP2, and 4EBP3 also correlated negatively with InsR (Table 2), and 4EBP1 and 4EBP2 correlated with plasma insulin levels (Table 2). None of the protein synthesis genes correlated with age.

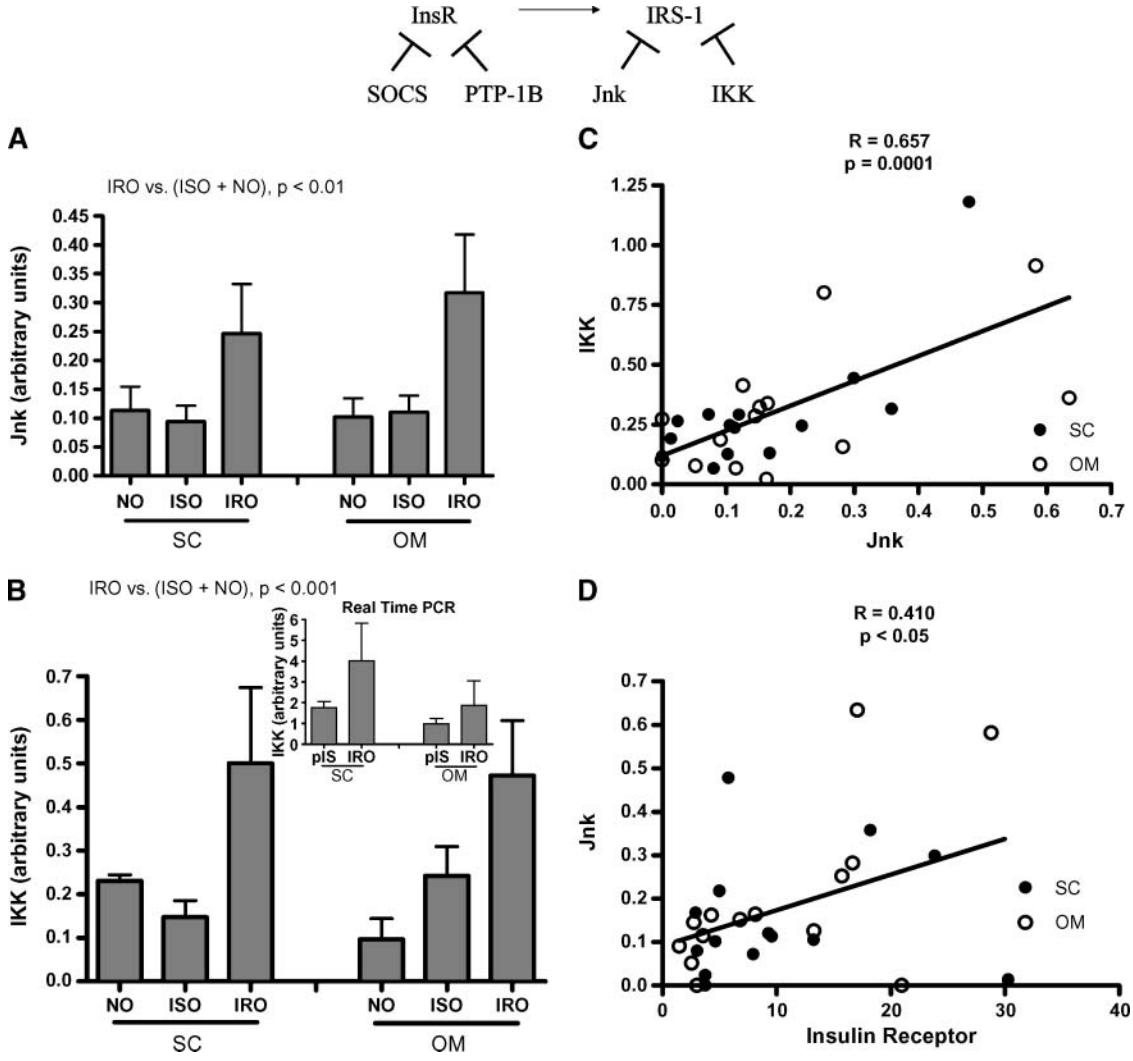

Fig. 3. IKK and Jnk, negative regulators of IRS-1, are upregulated in the IRO state. A, B: Gene expression of Jnk (A) and IKK (B) in SC and OM human adipose tissue from NO (n = 3–4), ISO (n = 5), and IRO (n = 5–6) subjects as assessed by CodeLink microarray. Confirmation of IKK gene expression by real-time TAQMAN PCR is shown in the inset in B. pIS, pooled insulin sensitive (NO + ISO). Data shown are means ± SEM. C, D: Correlation between IKK and Jnk (C) and Jnk and InsR (D) in pooled SC (closed circles) and OM (open circles) samples. Individual correlations in SC only and in OM only were all significant ($P = 0.02$ to $P < 0.001$), and SC and OM regression lines were not significantly different from each other in all cases.

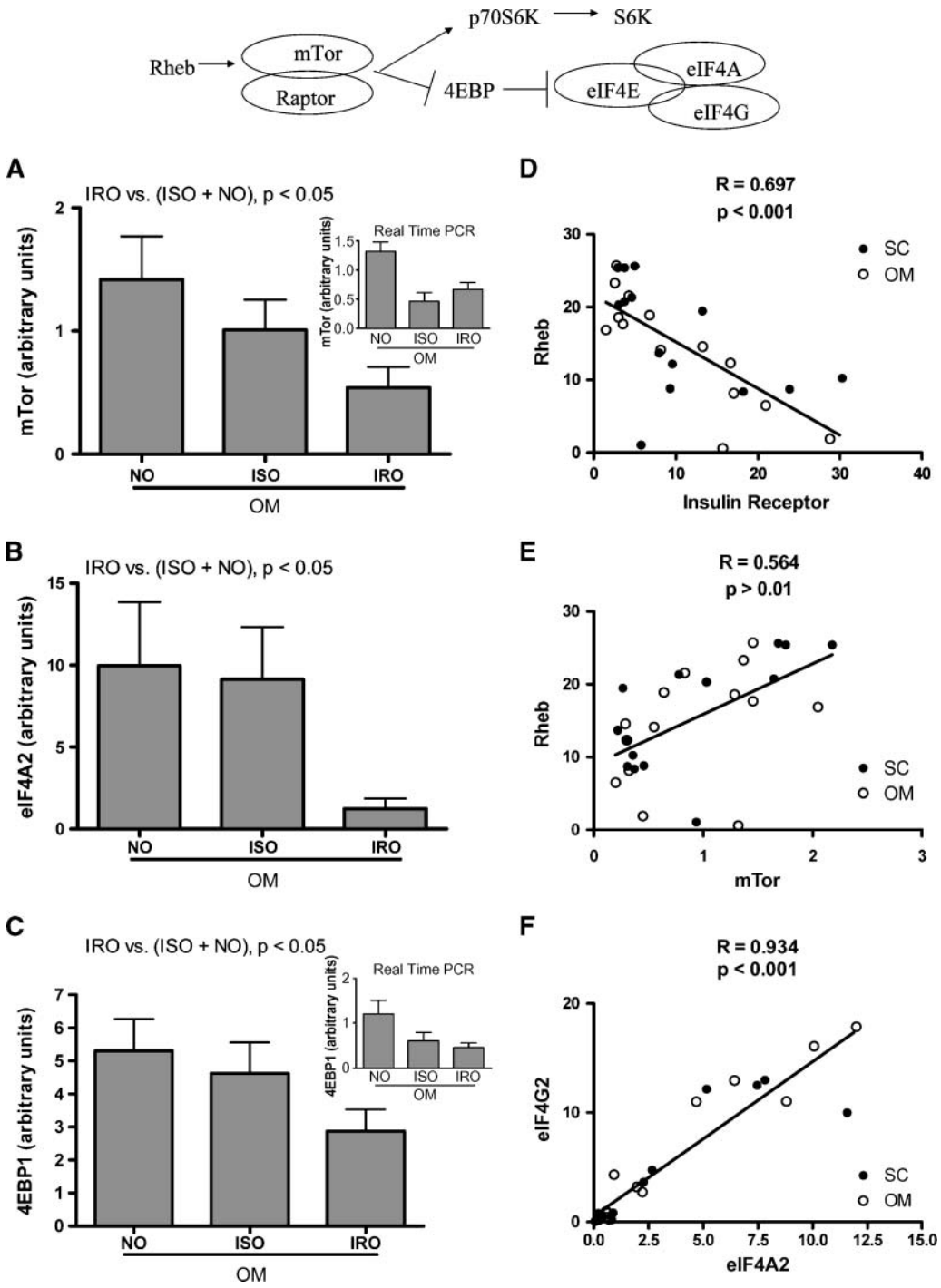

Fig. 4. In the protein synthesis pathway, mTor, Rheb, eIF4E, eIF4A1, eIF4A2, eIF4G2, 4EBP1, and 4EBP2 are altered in the IRO state. A–C: Gene expression of mTor (A), eIF4A2 (B), and 4EBP1 (C) in OM human adipose tissue from NO (n = 3), ISO (n = 5), and IRO (n = 6) subjects as assessed by CodeLink microarray. Confirmation of mTor gene expression by real-time TAQMAN PCR is shown in the inset in A, and confirmation of 4EBP1 by real-time TAQMAN PCR is shown in the inset in C. Data shown are means ± SEM. D–F: Correlations between Rheb and InsR (D), Rheb and mTor (E), and eIF4A2 and eIF4G2 (F) in pooled SC (closed circles) and OM (open circles) samples. Individual correlations in SC only and in OM only were all significant ($P < 0.05$ to $P < 0.0001$), and SC and OM regression lines were not significantly different from each other in all cases.

Proliferation pathway

The insulin signaling proliferation pathway includes SHC, GRB2, SOS, Ras, Raf-1, and MEK1/2 kinases (38). As shown in Table 2, by two-way paired ANOVA, expression of SHC (**Fig. 5A**; $P = 0.01$), SOS ($P = 0.022$), and Raf-1 ($P = 0.038$) all increased in the IRO group, whereas Ras ($P = 0.023$) and MEK1/2 kinase 1 (Fig. 5B; $P = 0.009$) decreased in the IRO group, with a similar trend with

TABLE 5. Pearson correlations within negative regulators of InsR and IRS-1

	PTP-1B	Jnk	IKK	Rheb	mTor	S6K
SOCS	0.342	0.313	0.341	−0.492	0.323	0.388
PTP-1B		0.371	0.622[a]	−0.485	0.237	0.611[a]
Jnk			0.589[a]	−0.554[a]	−0.403	0.709[b]
IKK				−0.775[c]	−0.257	0.703[b]
Rheb					0.434	−0.397
mTor						0.112

[a] $P < 0.05$.
[b] $P < 0.01$.
[c] $P < 0.001$.

MEK1/2 kinase 2. There were also several strong correlations within regulated genes in the proliferation pathway. As shown in Fig. 5C, D (SC and OM tissues) and in **Table 7** (OM tissue only), the correlations between SHC, SOS, Raf-1, and the MEK kinases are strong. Every gene in the proliferation pathway correlated with InsR (Table 2), with the exception of MEK1/2 kinase 2 (NS). Furthermore, SHC and SOS also correlated with plasma insulin levels (Table 2), whereas none of the genes correlated with age and only SHC correlated with BMI (Table 2). Note that, in multiple regression analysis ($r = 0.602$), in spite of forced entry of BMI into the equation (BMI $P = 0.03$), InsR ($P = 0.03$) still contributed significantly to predicting SHC.

Differentiation pathway

Differentiation genes specifically important to adipose tissue include the PPAR and CEBP families (39). Within the PPAR family, in SC and OM tissues together (two-way paired ANOVA; Table 2), PPARγ was significantly downregulated ($P = 0.014$; **Fig. 6A**), whereas two others were expressed at higher levels, PPARγ coactivator 1 ($P = 0.028$; Fig. 6A) and PPARδ ($P = 0.034$). In the CEBP family, CEBPγ (Fig. 6B; $P = 0.02$), CEBPβ (Fig. 6C; $P = 0.05$), CEBPε ($P = 0.0014$), and CEBPα ($P = 0.0019$) were all altered in the IRO group (Table 2; two-way paired ANOVA). The increased expression of CEBPγ in the IRO group was confirmed in all 28 samples for SC (data not shown) and OM (Fig. 6B, inset) using real-time PCR.

Several of the correlations within the PPAR family, within the CEBP family, and between the two families were striking. In OM tissue, PPARδ and PPARγ coactivator were positively correlated ($r = 0.838$, $P < 0.001$; **Table 8**); CEBPβ correlated strongly with CEBPα (Fig. 6D), and CEBPε and CEBPδ also correlate strongly (in OM tissue; $r = 0.702$, $P < 0.01$). Several strong correlations also existed between the InsR and the PPAR and CEBP families (Table 2, Fig. 6E–H). Fasting insulin levels were correlated with both PPARγ and PPARγ coactivator and also with CEBPε and CEBPα (Table 2). Age did not correlate with any of the differentiation genes (NS).

DISCUSSION

There are a number of limitations to this study. A large proportion of the samples were morbidly obese, limiting interpretations to that population. Furthermore, the measure of insulin sensitivity was limited to an evaluation of plasma insulin and HOMA from a single time point. Finally, there was no functional analysis of the adipose tissue. It should be noted that intact adipose tissue was chosen for the analysis. Although this tissue clearly represents a pool of adipocytes, preadipocytes, and macrophages, direct analysis of the tissue prevented the introduction of artifactual changes resulting from processing and separating the various cell populations. Hence, this can be viewed as both a strength and a limitation of the study.

There are two main strengths to this study: *i*) the inclusion of a range of subjects, which allowed for a simultaneous examination from lean to obese with a range in insulin sensitivity in both SC and OM adipose tissue; and *ii*) the use of a microarray, which allowed for the simultaneous measurement of the expression of multiple genes in the insulin signaling pathways. Not only did the design of this study allow for a comprehensive comparison of gene expression between SC and OM adipose tissue, it also allowed us to distinguish between changes in adipose tissue gene expression as a result of obesity versus insulin resistance.

We demonstrated that four commonly used housekeeping genes (32), HPRT1, TFRC, B2M, and PPIA, failed to reveal significant differences in the three groups, taking

TABLE 6. Pearson correlations within the protein synthesis pathway

	mTor	S6K	eIF4E	EIF4A1	EIF4A2	eIF4G1	eIF4G2	eIF4G3	4EBP1	4EBP2	4EBP3
Rheb	0.434	−0.397	0.600[a]	0.664[b]	0.697[b]	0.582[a]	0.676[b]	0.479	0.611[a]	0.479	0.723[b]
mTor		0.112	0.774[b]	0.724[b]	0.854[c]	0.006	0.831[c]	−0.271	0.157	0.200	0.148
S6K			0.212	0.059	−0.0126	−0.078	0.038	−0.375	−0.320	−0.355	−0.638[a]
eIF4E				0.827[c]	0.915[c]	0.516	0.927[c]	−0.005	0.187	0.0797	0.280
eIF4A1					0.862[c]	0.512	0.827[c]	0.233	0.398	0.012	0.369
eIF4A2						0.418	0.964[c]	0.049	0.300	0.197	0.349
eIF4G1							0.424	0.619[a]	0.364	−0.060	0.590[a]
eIF4G2								−0.022	0.321	0.302	0.386
eIF4G3									0.741[b]	−0.215	0.589[a]
4EBP1										0.156	0.693[b]
4EBP2											0.321

[a] $P < 0.05$.
[b] $P < 0.01$.
[c] $P < 0.001$.

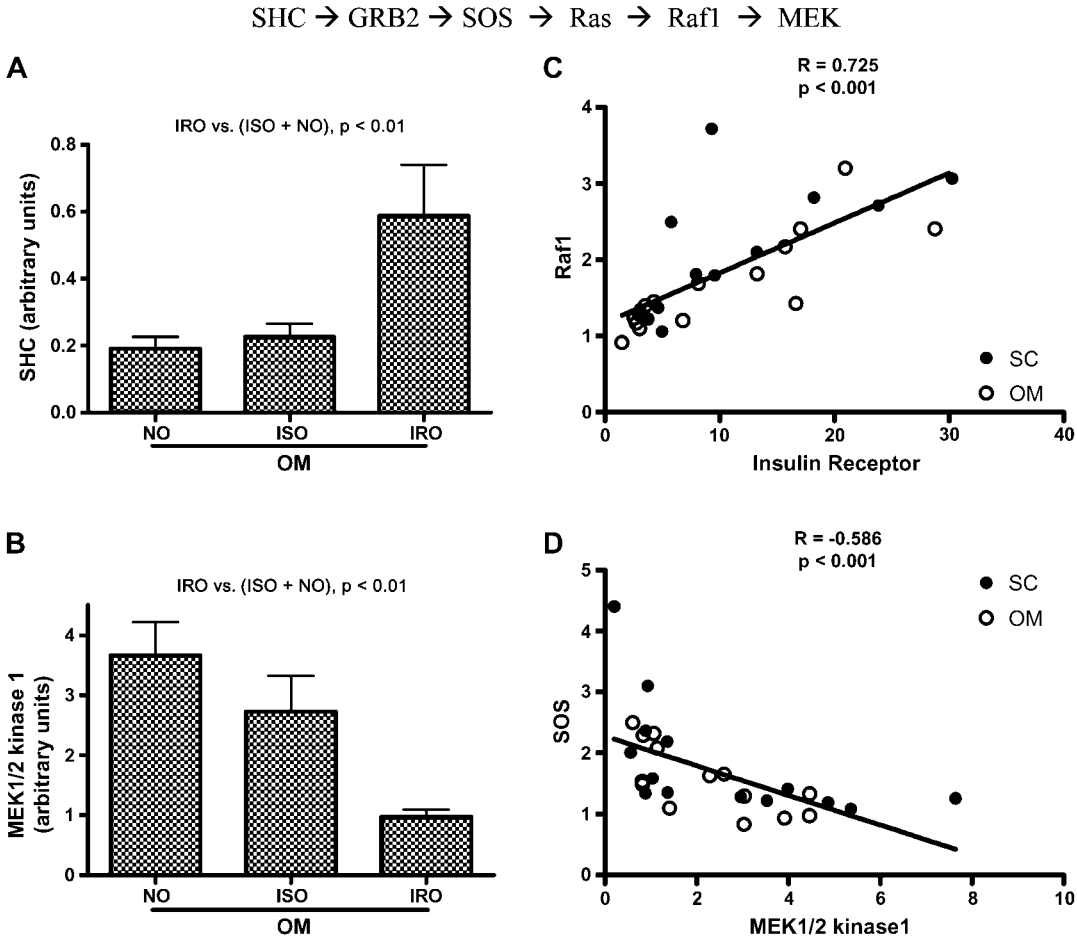

Fig. 5. In the proliferation pathway, SHC, SOS, Raf1, and MEK1/2 kinase 1 are altered in the IRO state. A, B: Gene expression of SHC (A) and MEK1/2 kinase 1 (B) in OM human adipose tissue from NO (n = 3), ISO (n = 5), and IRO (n = 6) subjects as assessed by CodeLink microarray. Data shown are means ± SEM. C, D: Correlations between Raf1 and InsR (C) and SOS and MEK1/2 kinase 1 (D) in pooled SC (closed circles) and OM (open circles) samples. Individual correlations in SC only and in OM only were all significant ($P = 0.02$ to $P = 0.0002$), and SC and OM regression lines were not significantly different from each other in all cases.

into account the two tissues, nor did they correlate with age, BMI, or insulin resistance. Furthermore, we confirmed one of these housekeeping genes, B2M, by real-time PCR, thus confirming the validity of the microarray technique.

The expression of almost all of the genes investigated, with the sole exception of IKK, was not different between the NO SC and NO OM tissues. Statistically, there was a global trend for insulin signaling genes to be regulated similarly in both tissues, although the differences were more pronounced in OM tissue. This greater change in the IRO group in OM tissue supports the premise that OM tissue is the more pertinent adipose tissue associated with metabolic disturbances (40).

Changes in adipose tissue insulin signaling gene expression were related to insulin sensitivity status much more than to obesity. Although other physiological differences may exist between NO and ISO populations beyond their BMI, the results of this study suggest that adipose tissue from ISO subjects more closely resembles the genetic profile from NO subjects and differs from

TABLE 7. Pearson correlations within the proliferation pathway

	GRB2	SOS	Ras	Raf1	MEK1/2 Kinase 1	MEK1/2 Kinase 2
SHC	0.213	0.838[a]	−0.546[b]	0.699[c]	−0.645[b]	−0.625[b]
GRB2		0.380	−0.042	0.506	−0.699[c]	0.270
SOS			−0.511	0.850[a]	−0.707[c]	−0.531[b]
Ras				−0.411	0.093	0.169
Raf1					−0.669[c]	−0.413
MEK1/2 kinase 1						0.381

[a] $P < 0.001$.
[b] $P < 0.05$.
[c] $P < 0.01$.

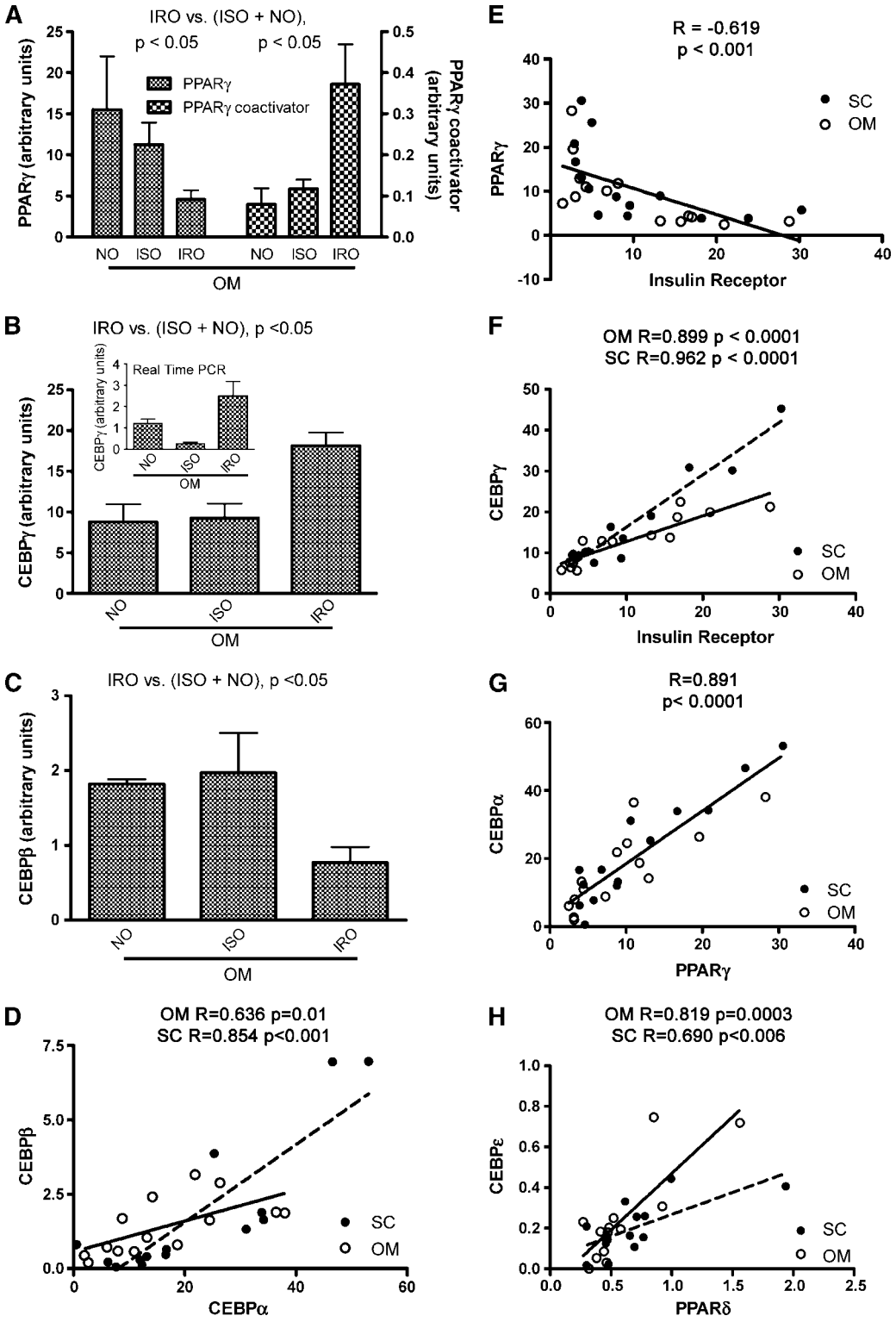

Fig. 6. In the differentiation pathway, PPARγ, PPARγ coactivator, PPARδ, CEBPβ, CEBPε, and CEBPγ are altered in the IRO state. Gene expression of PPARγ (left axis) and PPARγ coactivator (right axis) (A), CEBPγ (B), and CEBPβ (C) in OM human adipose tissue from NO (n = 3), ISO (n = 5), and IRO (n = 6) subjects as assessed by CodeLink microarray. Confirmation of CEBPγ gene expression by real time TAQMAN PCR is shown in the inset in B. Data shown are means ± SEM. E, G: Individual correlations between PPARγ and InsR (E) and CEBPα and PPARγ (G) in pooled SC (closed circles) and OM (open circles) samples. Individual correlations in SC only and in OM only were significant ($P = 0.02$ to $P < 0.0001$), and SC and OM regression lines were not significantly different from each other. D, F, H: Correlations between CEBPβ and CEBPα (D), CEBPγ and InsR (F), and CEBPε and PPARδ (H) for SC (closed circles, dotted lines) and OM (open circles, solid lines) samples. In each case, correlations were significant and positive, but regression lines for SC and OM were significantly different from each other.

TABLE 8. Pearson correlations within the differentiation pathway

	PPARδ	PPARγ Coactivator 1	CEBPε	CEBPα	CEBPβ	CEBPδ
PPARγ	−0.410	−0.444	−0.437	0.814[a]	0.606[b]	−0.278
PPARδ		0.838[a]	0.819[a]	−0.434	−0.506	0.583[b]
PPARγ coactivator 1			0.853[a]	−0.555[b]	−0.580[b]	0.761[c]
CEBPε				−0.456	−0.499	0.702[c]
CEBPα					0.636[b]	−0.447
CEBPβ						−0.139

[a] $P < 0.001$.
[b] $P < 0.05$.
[c] $P < 0.01$.

that of obese subjects who are insulin-resistant. This is true despite the fact of these two obese groups both being morbidly obese. This supports the hypothesis that obesity and insulin resistance can be distinct and separate risk factors for metabolic perturbances (41). Furthermore, we have shown that the presence of obesity does not necessarily cause the altered gene changes. Although obesity is related to insulin resistance, it is not necessarily associated with insulin resistance.

Changes in gene expression in the IRO subjects were present in all of the insulin signaling pathways investigated. Within each pathway, the expression of several genes was disrupted; furthermore, alterations were specific to key isoforms of the genes and did not result in all genes being altered. The disruption of so many insulin-related genes in adipocyte pathways related to glucose transport, protein synthesis, regulatory genes, proliferation, and differentiation demonstrated a dramatic shift in the state of adipose tissue in IRO subjects.

The central genes, implicated in all insulin signaling pathways, are InsR and IRS-1. There was a striking similarity in the changes in these two genes. Regardless of body size, insulin sensitivity, or tissue (SC or OM), these two genes followed a strikingly similar pattern, as demonstrated by the correlation between the two genes. Furthermore, genes from each of the other pathways investigated were found to change in close concert (significantly positive or negative) with InsR and IRS-1, further supporting a global shift in the readiness status (as indicated by mRNA changes) of the adipose tissue. Interestingly, the negative regulators of IRS-1, Jnk and IKK, were both upregulated in the IRO state, supporting the hypothesis that these inflammation-related genes contribute to insulin resistance (42). However, notwithstanding the apparent physiological indication of insulin resistance in the IRO subjects (as suggested by the increased glucose, insulin, and HOMA index), the increased expression levels of InsR, IRS-1, and GLUT4 were indicative of a compensatory mechanism. Although GLUT4 protein and function were not measured in the present study, previous data from Marette et al. (43) support the idea that adipose tissue remains insulin-sensitive even in severely obese insulin-resistant subjects, as shown by active insulin stimulation of glucose transport in both SC and OM adipose tissue and by a positive correlation of GLUT4 mRNA with insulin (43).

In IRO subjects, a general pattern emerged that potentially reflects a limitation on adipose growth. Montague et al. (44) found a strong negative correlation between adipocyte PPARγ expression and BMI. They suggested that the decreased PPARγ expression may be an attempt by the adipocyte to restrain fat accumulation and/or may simply be indicative of the cells being large and insulin-resistant. Our data show that, in spite of increases in PPARγ coactivator and CEBPγ, in IRO subjects, the expression of not only PPARγ but also CEBPβ, and all of the altered protein synthesis and glucose signaling pathways, is downregulated. CEBPβ is an early marker of differentiation, but it also functions later in differentiation to induce CEBPα, which stimulates differentiation along with PPARγ (45). The expression of these genes, however, did not correlate with BMI in our subject groups, because in the ISO group, despite being morbidly obese, the gene expression was not different from that in the NO group in each case. Thus, the resulting correlation between BMI and these genes in our study was not significant. However, the decreased expression in the IRO group versus the NO group does agree with the findings of Montague et al. (44), underscoring the importance of recognizing the ISO population and its unique physiology. Therefore, a decrease in glucose transport, protein synthesis, and differentiation genes may reflect an attempt of the adipocyte to restrain growth.

We further speculate that the increase in the proliferation genes, SHC and raf-1, reflects an attempt to remodel adipose tissue with smaller adipocytes. Although this is only speculation, the IRO subjects, although obese and having high fasting insulin, have not been diagnosed with non-insulin-dependent diabetes mellitus (NIDDM). It has been reported that adipocytes from NIDDM subjects are larger and less able to trap circulating lipids (46). It was suggested previously that alterations in adipose tissue may precede NIDDM, that adipose tissue may be the first tissue to demonstrate insulin intolerance, and that such alterations may be able to initiate insulin resistance in other peripheral tissues (47). The changes observed here in the gene expression of several key insulin signaling pathways in obese subjects may reflect the changes that first develop with insulin intolerance and the compensatory changes that the adipocyte may use.

Finally, it is interesting that PPARδ expression was increased in our IRO group. Until recently, little was known regarding the function of PPARδ, but Takahashi and

colleagues (48), in a recent review, proposed that the main function of PPARδ may be to switch the adipocyte from glucose metabolism to fatty acid metabolism and that antagonists may be beneficial in combating metabolic syndrome. The upregulation of PPARδ in adipose tissue of IRO subjects further supports the idea that the adipocyte cells have altered metabolic gene expression levels to compensate for the local development of insulin resistance.

Further investigation into other differences between NO, ISO, and IRO populations may lead to better understanding of the changes that occur in the development of obesity when insulin resistance is not present and a confounding factor. Here, we have demonstrated that important changes in the expression level of key genes in many insulin signaling pathways occur in OM tissue with the development of insulin resistance rather than obesity.

This work was supported by Grant MOP64446 from Canadian Institutes of Health Research to K.C., who holds a Canada Research Chair in Adipose Tissue. R.M. was supported by a scholarship from the Natural Sciences and Engineering Research Council of Canada. The authors appreciate the helpful suggestions and constructive criticism of Dr. Robert Sladek (Montreal Genomics and Proteomics Centre, McGill University Health Centre, Montreal, Canada) for the microarray analysis.

REFERENCES

1. Alberti, K. G., and P. Z. Zimmet. 1998. Definition, diagnosis and classification of diabetes mellitus and its complications. I. Diagnosis and classification of diabetes mellitus provisional report of a WHO consultation. *Diabet. Med.* **15:** 539–553.
2. Haffner, S. M. 2006. Relationship of metabolic risk factors and development of cardiovascular disease and diabetes. *Obesity.* **14 (Suppl. 3):** 121–127.
3. Despres, J. P., and I. Lemieux. 2006. Abdominal obesity and metabolic syndrome. *Nature.* **444:** 881–887.
4. Reaven, G. 2005. All obese individuals are not created equal: insulin resistance is the major determinant of cardiovascular disease in overweight/obese individuals. *Diabetes Vasc. Dis. Res.* **2:** 105–112.
5. Reaven, G., F. Abbasi, and T. McLaughlin. 2004. Obesity, insulin resistance, and cardiovascular disease. *Recent Prog. Horm. Res.* **59:** 207–223.
6. Sims, E. A. 2001. Are there persons who are obese, but metabolically healthy? *Metabolism.* **50:** 1499–1504.
7. St. Pierre, D. H., A. D. Karelis, L. Coderre, F. Malita, J. Fontaine, D. Mignault, M. Brochu, J. P. Bastard, K. Cianflone, E. Doucet, et al. 2007. Association of acylated and nonacylated ghrelin with insulin sensitivity in overweight and obese postmenopausal women. *J. Clin. Endocrinol. Metab.* **92:** 264–269.
8. Karelis, A. D., D. H. St. Pierre, F. Conus, R. Rabasa-Lhoret, and E. T. Poehlman. 2004. Metabolic and body composition factors in subgroups of obesity: what do we know? *J. Clin. Endocrinol. Metab.* **89:** 2569–2575.
9. Brochu, M., A. Tchernof, I. J. Dionne, C. K. Sites, G. H. Eltabbakh, E. A. Sims, and E. T. Poehlman. 2001. What are the physical characteristics associated with a normal metabolic profile despite a high level of obesity in postmenopausal women? *J. Clin. Endocrinol. Metab.* **86:** 1020–1025.
10. Karelis, A. D., M. Brochu, R. Rabasa-Lhoret, D. Garrel, and E. T. Poehlman. 2004. Clinical markers for the identification of metabolically healthy but obese individuals. *Diabetes Obes. Metab.* **6:** 456–457.
11. Lim, S. C., B. Y. Tan, S. K. Chew, and C. E. Tan. 2002. The relationship between insulin resistance and cardiovascular risk factors in overweight/obese non-diabetic Asian adults: the 1992 Singapore National Health Survey. *Int. J. Obes. Relat. Metab. Disord.* **26:** 1511–1516.
12. Shin, M. J., Y. J. Hyun, O. Y. Kim, J. Y. Kim, Y. Jang, and J. H. Lee. 2006. Weight loss effect on inflammation and LDL oxidation in metabolically healthy but obese (MHO) individuals: low inflammation and LDL oxidation in MHO women. *Int. J. Obes.* **30:** 1529–1534.
13. Eriksson, J. W., U. Smith, F. Waagstein, M. Wysocki, and P. A. Jansson. 1999. Glucose turnover and adipose tissue lipolysis are insulin-resistant in healthy relatives of type 2 diabetes patients: is cellular insulin resistance a secondary phenomenon? *Diabetes.* **48:** 1572–1578.
14. Laviola, L., S. Perrini, A. Cignarelli, A. Natalicchio, A. Leonardini, F. De Stefano, M. Cuscito, M. De Fazio, V. Memeo, V. Neri, et al. 2006. Insulin signaling in human visceral and subcutaneous adipose tissue in vivo. *Diabetes.* **55:** 952–961.
15. Bolinder, J., L. Kager, J. Ostman, and P. Arner. 1983. Differences at the receptor and postreceptor levels between human omental and subcutaneous adipose tissue in the action of insulin on lipolysis. *Diabetes.* **32:** 117–123.
16. Maslowska, M. H., A. D. Sniderman, L. D. MacLean, and K. Cianflone. 1993. Regional differences in triacylglycerol synthesis in adipose tissue and in cultured preadipocytes. *J. Lipid Res.* **34:** 219–228.
17. Hube, F., M. Birgel, Y. M. Lee, and H. Hauner. 1999. Expression pattern of tumour necrosis factor receptors in subcutaneous and omental human adipose tissue: role of obesity and non-insulin-dependent diabetes mellitus. *Eur. J. Clin. Invest.* **29:** 672–678.
18. Hube, F., U. Lietz, M. Igel, P. B. Jensen, H. Tornqvist, H. G. Joost, and H. Hauner. 1996. Difference in leptin mRNA levels between omental and subcutaneous abdominal adipose tissue from obese humans. *Horm. Metab. Res.* **28:** 690–693.
19. Williams, L. B., R. L. Fawcett, A. S. Waechter, P. Zhang, B. E. Kogon, R. Jones, M. Inman, J. Huse, and R. V. Considine. 2000. Leptin production in adipocytes from morbidly obese subjects: stimulation by dexamethasone, inhibition with troglitazone, and influence of gender. *J. Clin. Endocrinol. Metab.* **85:** 2678–2684.
20. Richelsen, B., S. B. Pedersen, T. Moller-Pedersen, and J. F. Bak. 1991. Regional differences in triglyceride breakdown in human adipose tissue: effects of catecholamines, insulin, and prostaglandin E2. *Metabolism.* **40:** 990–996.
21. Dicker, A., M. Ryden, E. Naslund, I. E. Muehlen, M. Wiren, M. Lafontan, and P. Arner. 2004. Effect of testosterone on lipolysis in human pre-adipocytes from different fat depots. *Diabetologia.* **47:** 420–428.
22. Hoffstedt, J., P. Arner, G. Hellers, and F. Lonnqvist. 1997. Variation in adrenergic regulation of lipolysis between omental and subcutaneous adipocytes from obese and non-obese men. *J. Lipid Res.* **38:** 795–804.
23. James, W. P., N. Rigby, and R. Leach. 2006. Obesity and the metabolic syndrome: the stress on society. *Ann. N. Y. Acad. Sci.* **1083:** 1–10.
24. Lefebvre, A. M., M. Laville, N. Vega, J. P. Riou, L. van Gaal, J. Auwerx, and H. Vidal. 1998. Depot-specific differences in adipose tissue gene expression in lean and obese subjects. *Diabetes.* **47:** 98–103.
25. Capeau, J. 2003. [Insulin signaling: mechanisms altered in insulin resistance.] *Med. Sci. (Paris).* **19:** 834–839.
26. Kido, Y., J. Nakae, and D. Accili. 2001. Clinical review 125. The insulin receptor and its cellular targets. *J. Clin. Endocrinol. Metab.* **86:** 972–979.
27. Jones, K. L., S. S. King, and M. J. Iqbal. 2004. Endophyte-infected tall fescue diet alters gene expression in heifer luteal tissue as revealed by interspecies microarray analysis. *Mol. Reprod. Dev.* **67:** 154–161.
28. Tusher, V. G., R. Tibshirani, and G. Chu. 2001. Significance analysis of microarrays applied to the ionizing radiation response. *Proc. Natl. Acad. Sci. USA.* **98:** 5116–5121.
29. Karelis, A. D., M. Brochu, and R. Rabasa-Lhoret. 2004. Can we identify metabolically healthy but obese individuals (MHO)? *Diabetes Metab.* **30:** 569–572.
30. Sucharda, P. 1989. [Clinical significance of the quantification of obesity. The Quetelet index and its use.] *Cas. Lek. Cesk.* **128:** 1040–1043.
31. Expert Committee. 2003. Report of the Expert Committee on the Diagnosis and Classification of Diabetes Mellitus. *Diabetes Care.* **26 (Suppl.):** 5–20.
32. Gorzelniak, K., J. Janke, S. Engeli, and A. M. Sharma. 2001. Validation of endogenous controls for gene expression studies

in human adipocytes and preadipocytes. *Horm. Metab. Res.* **33:** 625–627.
33. Zhou, Q. L., J. G. Park, Z. Y. Jiang, J. J. Holik, P. Mitra, S. Semiz, A. Guilherme, A. M. Powelka, X. Tang, J. Virbasius, et al. 2004. Analysis of insulin signalling by RNAi-based gene silencing. *Biochem. Soc. Trans.* **32:** 817–821.
34. Shi, K., K. Egawa, H. Maegawa, T. Nakamura, S. Ugi, Y. Nishio, and A. Kashiwagi. 2004. Protein-tyrosine phosphatase 1B associates with insulin receptor and negatively regulates insulin signaling without receptor internalization. *J. Biochem. (Tokyo).* **136:** 89–96.
35. Ueno, M., J. B. Carvalheira, R. C. Tambascia, R. M. Bezerra, M. E. Amaral, E. M. Carneiro, F. Folli, K. G. Franchini, and M. J. Saad. 2005. Regulation of insulin signalling by hyperinsulinaemia: role of IRS-1/2 serine phosphorylation and the mTOR/p70 S6K pathway. *Diabetologia.* **48:** 506–518.
36. Hiratani, K., T. Haruta, A. Tani, J. Kawahara, I. Usui, and M. Kobayashi. 2005. Roles of mTOR and JNK in serine phosphorylation, translocation, and degradation of IRS-1. *Biochem. Biophys. Res. Commun.* **335:** 836–842.
37. El Chaar, D., A. Gagnon, and A. Sorisky. 2004. Inhibition of insulin signaling and adipogenesis by rapamycin: effect on phosphorylation of p70 S6 kinase vs eIF4E–BP1. *Int. J. Obes. Relat. Metab. Disord.* **28:** 191–198.
38. Skolnik, E. Y., C. H. Lee, A. Batzer, L. M. Vicentini, M. Zhou, R. Daly, M. J. Myers, Jr., J. M. Backer, A. Ullrich, and M. F. White. 1993. The SH2/SH3 domain-containing protein GRB2 interacts with tyrosine-phosphorylated IRS1 and Shc: implications for insulin control of ras signalling. *EMBO J.* **12:** 1929–1936.
39. Rosen, E. D. 2005. The transcriptional basis of adipocyte development. *Prostaglandins Leukot. Essent. Fatty Acids.* **73:** 31–34.
40. Seidell, J. C., J. G. Hautvast, and P. Deurenberg. 1989. Overweight: fat distribution and health risks. Epidemiological observations. A review. *Infusionstherapie.* **16:** 276–281.
41. McLaughlin, T., G. Allison, F. Abbasi, C. Lamendola, and G. Reaven. 2004. Prevalence of insulin resistance and associated cardiovascular disease risk factors among normal weight, overweight, and obese individuals. *Metabolism.* **53:** 495–499.
42. Nguyen, M. T., H. Satoh, S. Favelyukis, J. L. Babendure, T. Imamura, J. I. Sbodio, J. Zalevsky, B. I. Dahiyat, N. W. Chi, and J. M. Olefsky. 2005. JNK and tumor necrosis factor-alpha mediate free fatty acid-induced insulin resistance in 3T3-L1 adipocytes. *J. Biol. Chem.* **280:** 35361–35371.
43. Marette, A., P. Mauriege, B. Marcotte, C. Atgie, C. Bouchard, G. Theriault, L. J. Bukowiecki, P. Marceau, S. Biron, A. Nadeau, et al. 1997. Regional variation in adipose tissue insulin action and GLUT4 glucose transporter expression in severely obese premenopausal women. *Diabetologia.* **40:** 590–598.
44. Montague, C. T., J. B. Prins, L. Sanders, J. Zhang, C. P. Sewter, J. Digby, C. D. Byrne, and S. O'Rahilly. 1998. Depot-related gene expression in human subcutaneous and omental adipocytes. *Diabetes.* **47:** 1384–1391.
45. Lane, M. D., Q. Q. Tang, and M. S. Jiang. 1999. Role of the CCAAT enhancer binding proteins (C/EBPs) in adipocyte differentiation. *Biochem. Biophys. Res. Commun.* **266:** 677–683.
46. Heilbronn, L., S. R. Smith, and E. Ravussin. 2004. Failure of fat cell proliferation, mitochondrial function and fat oxidation results in ectopic fat storage, insulin resistance and type II diabetes mellitus. *Int. J. Obes. Relat. Metab. Disord.* **28 (Suppl. 4):** 12–21.
47. Smith, U. 2002. Impaired ('diabetic') insulin signaling and action occur in fat cells long before glucose intolerance—is insulin resistance initiated in the adipose tissue? *Int. J. Obes. Relat. Metab. Disord.* **26:** 897–904.
48. Takahashi, S., T. Tanaka, T. Kodama, and J. Sakai. 2006. Peroxisome proliferator-activated receptor delta (PPARdelta), a novel target site for drug discovery in metabolic syndrome. *Pharmacol. Res.* **53:** 501–507.